Programmed Materials Synthesis with DNA

James J. Storhoff and Chad A. Mirkin*

Department of Chemistry, Northwestern University, Evanston, Illinois 60208

Received October 19, 1998 (Revised Manuscript Received February 24, 1999)

Contents

I. Introduction

Learning how to control the formation and two- and three-dimensional assembly of molecular scale building blocks into well-defined meso- and macroscopic structures is the essence of nanotechnology and materials chemistry. DNA is arguably one of the most programmable "assemblers" available to the synthetic chemist and materials scientist, yet until recently, it has been an underutilized synthon in materials chemistry. The purpose of this review is to summarize advances made involving new strategies that rely on the use of both naturally occurring DNA and synthetic oligonucleotides to assemble nanoscale nonbiological building blocks into extended meso- and macroscopic structures. Although early in their development, some of these strategies already have been shown to be useful in generating novel nanostructured materials,[1−4] arranging inorganic nanoparticles into "anatural" configurations,[5,6] understanding interparticle electronic interactions,[1] templating the growth of nanocircuitry,[7] and developing a promising new detection technology for DNA.[8,9]

There are two basic types of building blocks that are applicable to a variety of assembly schemes: molecules with synthetically programmed recognition sites or bits of matter with nanoscale dimensions and well-defined surface chemistries. The latter type of building block is often referred to as a "nanoparticle" or "nanocrystal". Assembly of such building blocks into extended, well-defined structures can provide a variety of functional materials with applications including ultrasmall electronic devices,[10−13] spectroscopic enhancers,[14,15] high-density information storage media,[16,17] and highly sensitive and selective chemical detectors.[8,9,18] The assembly of nanoparticle and molecular building blocks into functional structures has been accomplished through both physical and chemical methods.[19] Physical methods include the use of scanning probe microscopy,[20−22] electrophoretic strategies,[23,24] LB films,[25,26] or template-driven sedimentation[27] to position particles in a preconceived fashion within a matrix or on a substrate. Although effective for preparing certain types of nanoscale architectures, many of these physical methods are limited because they are often slow and do not lend themselves to preparing designed nanostructured architectures that canvas macroscopic dimensions. Chemical methods include ordering particles based upon interparticle electrostatic interactions,[28−30] covalent assembly,[31,32] template recognition,[33,34] template recognition with subsequent covalent cross-linking reactions,[35,36] crystallization based upon weak intermolecular interactions,[37−41] or linking reactions involving designed organic or biological recognition sites.[1,2,4,42] The advantages of chemical methods are that building block linking processes can occur in a massively parallel fashion and in some cases possess self-annealing or correcting properties. This makes them particularly attractive for constructing two- and three-dimensional structures on a faster time scale. The disadvantage is that at present chemical methods, when compared with some of the aforementioned physical deposition methods, are difficult to control.

Recently, there has been substantial interest in utilizing biomolecules to direct the formation of extended meso- and macroscopic architectures.[43,44] The advantage of using biomolecules is that molecular recognition is already built into the building block of interest (e.g., peptides, oligonucleotides, and proteins). In some cases, synthetic versions of the biomolecules are readily available and easily adaptable to both inorganic and organic building blocks and substrates.[45]

This review examines the use of one class of these biomolecules, DNA, to organize nanometer-sized structures into preconceived extended, functional structures and materials. It is divided into three categories; the use of (1) oligonucleotides (single-stranded DNA) to prepare meso- and macroscopic *organic* structures, (2) duplex DNA as a physical template for growing inorganic wires and organizing nonbiological building blocks into extended hybrid materials, and (3) oligonucleotide functionalized nanoparticles and sequence-specific hybridization reactions for organizing such particles into periodic, functional structures.

10.1021/cr970071p CCC: $35.00
Published on Web 06/04/1999

James Storhoff was born on July 13, 1973, in Muncie, IN. He received his B.S. degree in chemistry from Ball State University in 1995 and his M.S. degree in chemistry from Northwestern University in 1996. He is currently pursuing his Ph.D. in chemistry at Northwestern University under the direction of Professor Chad Mirkin. He was co-recipient of the 1998 BFGoodrich Collegiate Inventors Award. His research interests fall in the general area of biomaterials chemistry.

Chad Mirkin received his B.S. from Dickinson College in 1986 and his Ph.D. in chemistry from The Pennsylvania State University in 1989. In the same year he became an NSF Postdoctoral Fellow at MIT. He joined the faculty of Northwestern University in 1991, and in 1997 he assumed the Charles E. and Emma H. Morrison Professorship of Chemistry. Mirkin's multidisciplinary research program focuses on the interfaces of organometallic, surface, and electrochemistry. His main research interests are (1) surface coordination chemistry and design, (2) nanotechnology, (3) sensor development, and (4) the rational design of hybrid ligands for electrochemically controlling transition metal stoichiometric and catalytic reactivity. Mirkin's honors include the 1999 MRS Young Investigator Award, the 1999 ACS Award in Pure Chemistry, the 1998 Phi Lambda Upsilon Fresenius Award, the 1998 E. Bright Wilson Prize (Harvard University), the 1998 BFGoodrich Collegiate Inventors Award, the Camille Dreyfus Teacher-Scholar Award, the Alfred P. Sloan Foundation Award, the DuPont Young Professor Award, the NSF Young Investigator Award, the Beckman Young Investigator Award, and the Camille and Henry Dreyfus Foundation New Faculty Award. Professor Mirkin is the author or co-author of over 80 publications and 8 patents and is an active consultant with several major chemical companies.

II. Meso- and Macroscopic Organic Structures from DNA

Advances in oligonucleotide synthesis and subsequent modification have paved the way for the use of DNA as a tool in materials applications.[45] DNA's unique molecular recognition properties and scaffold-like structure, combined with the straightforward preparatory methods for modifying DNA, provide many opportunities for the construction of meso- and macroscopic periodic arrays from both inorganic and organic building blocks.

Scheme 1[a]

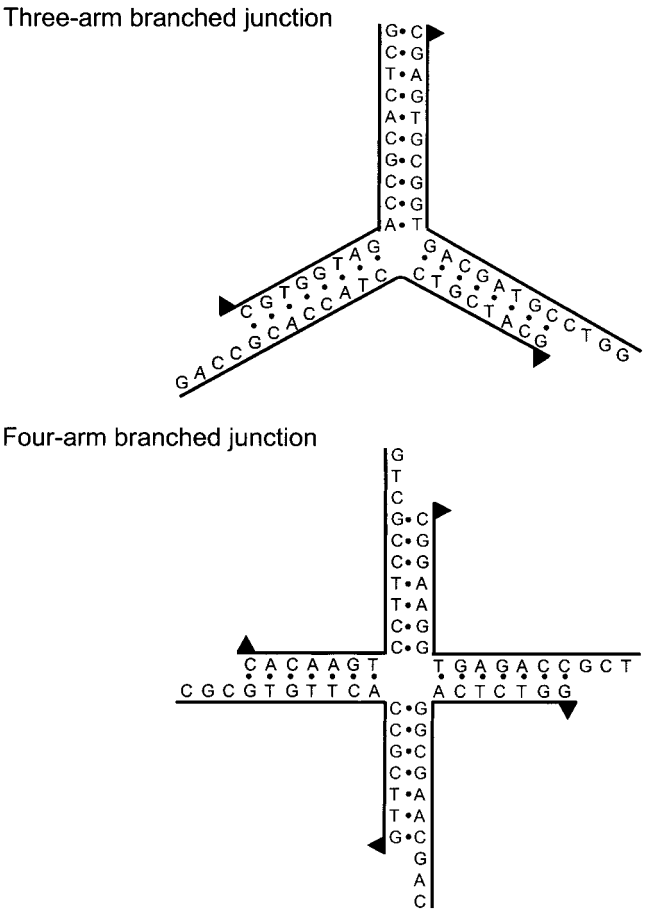

[a] Top: reprinted with permission from ref 49. Copyright 1986 Oxford University Press. Bottom: reprinted with permission from ref 48. Copyright 1983 Macmillan Magazines Limited.

Seeman and co-workers were the first to exploit DNA's molecular recognition properties to design complex mesoscopic structures based solely on DNA.[44,46] Their first entry into this area was the preparation of branched junctions that serve as building blocks for more complex two- and three-dimensional DNA structures, Scheme 1. These junctions are stable analogues to Holliday junctions, which are transient branched DNA intermediates observed in DNA replication.[47] Three- and four-arm branched junctions have been prepared through appropriate sequence design, hybridization conditions, and annealing procedures.[48,49] Five- and six-arm branched junctions also have been realized, although these structures require longer DNA "arms" because of increased instability at their vertices.[50] By placing single-stranded "sticky ends" on the arms of these branched DNA building blocks (Scheme 1), more complex two- and three-dimensional DNA structures can be prepared. In these structures, the edges are comprised of double-stranded DNA while the vertices are formed by the junctions. One of the first and most elementary structures to be synthesized in this manner was a DNA quadrilateral based on the assembly of four complementary three-arm branched junctions through the association of sequence-specific sticky ends, Scheme 2.[51] Once these

Scheme 2

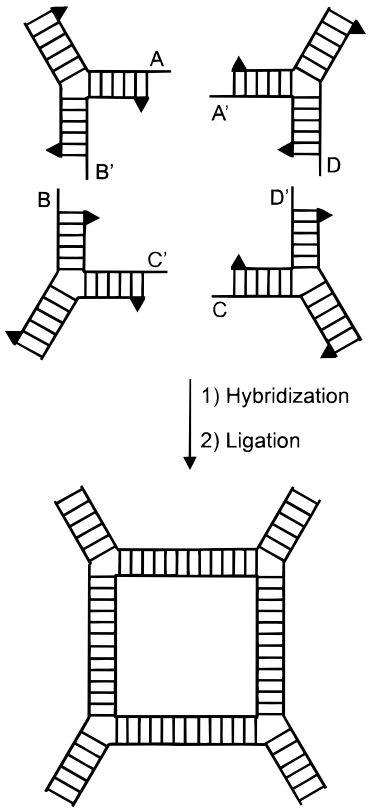

structures are formed, DNA ligase[52] can be used to covalently link the "nicks" in the DNA within these structures, providing a more rigid scaffolding material. It is important to note that since these structures possess flexible junctions,[49] the geometric assignment relies on *topology* and not actual geometry. In principle, by controlling the number of "arms" in a given branched DNA structure, the connectivities of more complex DNA structures can be controlled. However, thus far it has proven very difficult to synthesize more complex three-dimensional structures in solution because of low yields (e.g., 15% for the quadrilateral). For example, although a DNA hexacatenane with the connectivity of a cube has been prepared, it was isolated in only ~1% yield.[53]

Seeman and co-workers recently developed a solid-support methodology for preparing DNA materials to help overcome the problems (i.e., low yield, purification) associated with their solution-based methods.[54] With this approach, the yields were significantly increased and more complex structures that could not be synthesized in solution became accessible. One example is the construction of a DNA truncated octahedron containing 2550 nucleotides with an estimated molecular weight of 790 kDa.[55] By comparison, the DNA cube, which was the most complex structure synthesized in solution, contains 540 nucleotides. The reader is referred to a recent review by Seeman for further details on the design, synthesis, and characterization of these fascinating materials.[56]

These initial structures demonstrated that the molecular recognition properties of DNA, in conjunction with enzymatic ligation, could be used to construct complex structures based on DNA. However, one of the main drawbacks of this strategy is the lack of rigidity at the vertices of the resulting structures, which is a consequence of the branched DNA building blocks used in their preparation. This limits the potential use of these materials as physical templates for organizing other materials (i.e., proteins, nanoscale inorganic and organic building blocks) into well-defined, three-dimensional structures. In addition, it is very difficult to characterize these materials which are comprised solely of DNA; to date characterization methods have involved extensive use of restriction enzymes, ligation, and gel electrophoresis.[49] Nevertheless, this work is an impressive demonstration of the synthetic control possible through the use of oligonucleotide synthons and the relatively simple base-pairing rules that govern the hybridization properties of DNA.

To overcome the problem of DNA flexibility, Seeman and co-workers have recently employed DNA double-crossover molecules (referred to as DX molecules by Seeman) as building blocks[57,58] for the assembly of two-dimensional DNA crystals, Scheme 3.[59] DX molecules are branched DNA molecules that contain two crossover sites between helical domains. Two classes of these molecules have been prepared and are distinguished by the relative orientations of the oligonucleotide strands that comprise them.[57,58] The two classes of molecules are referred to as "parallel" (DP) and "antiparallel" (DA). In this review, the focus will be solely on the DA class of DX molecules because of their superior mechanical properties.[58] The two DA molecules discussed herein are referred to as "DAE" and "DAO" molecules and differ by the number of DNA strands per complex and the number of helical turns between the two crossover points. The "DAE" molecules possess an even (E) number of half-turns between the crossover points, while the "DAO" molecules possess an odd (O) number of half-turns. As shown in Scheme 3B, the "DAE" molecules are prepared from five strands of DNA and possess one full turn of DNA between the crossover points (circled in Scheme 3B). The "DAO" molecules are constructed from only four strands of DNA and possess one and a half full turns of DNA between the crossover points. Unlike the very flexible branched junctions discussed previously, both the DAE and DAO branched DNA building blocks have a rigidity comparable to linear duplex DNA,[58] which makes them ideal building blocks for the construction of DNA-based materials with identifiable and rationally designable structures. In addition, using gel electrophoresis, the researchers have shown that ≥95% of the DX material generated appears in a single band. By using two DAE (or DAO, not shown here) molecules (**A** and **B**) with complementary "sticky ends" at the four edges of these structures, which are synthetically programmed to form a two-dimensional lattice (note "slipped" design in Scheme 3A), two-dimensional periodic arrays of DNA as large as $2 \times 8\ \mu$m were formed and characterized by atomic force microscopy (AFM).[59] By using a "reporter" DAE molecule (**B′**) containing a hairpin sequence that could be imaged by AFM, the periodicities of the two-dimensional lattices were determined by measuring

Scheme 3[a]

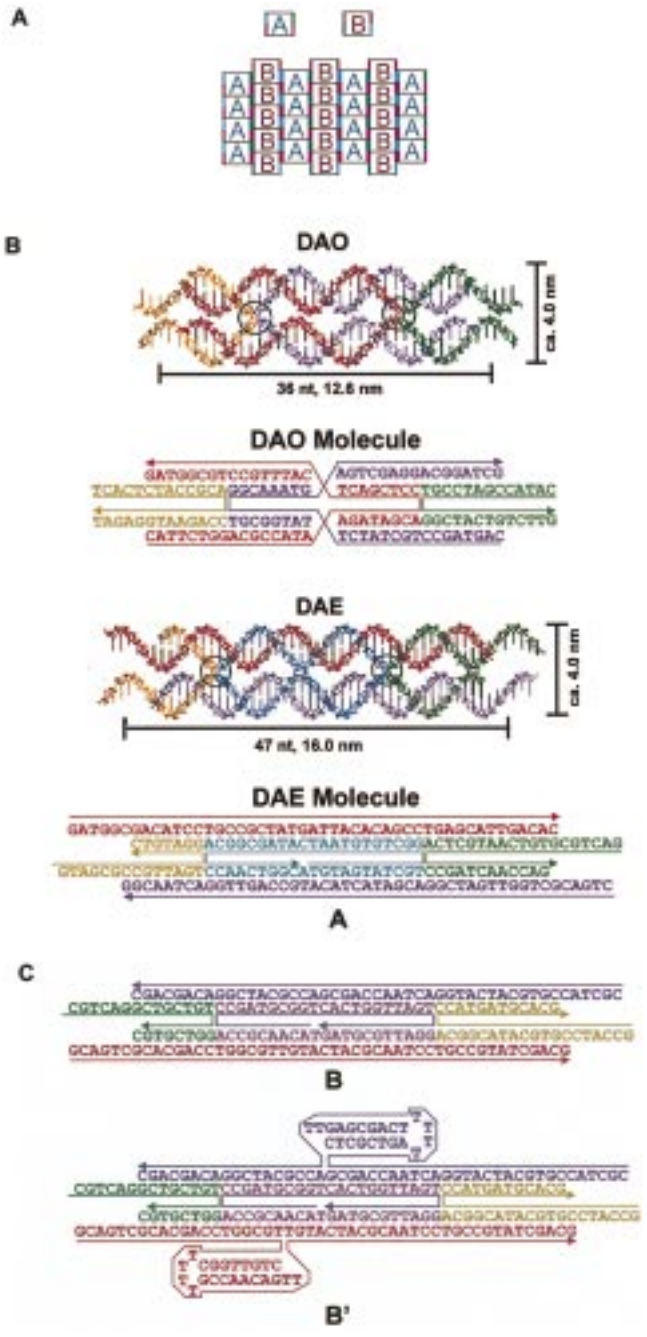

[a] Reprinted with permission from ref 59. Copyright 1998 Macmillan Magazines Limited.

the distance between the "stripes" located within the lattice, which represent the hairpin structures, Scheme 3 and Figure 1. The periodicity of the two-dimensional lattices that were imaged (33 ± 3 nm) correlated very well with the calculated periodicity (32 nm) based on the length of the DAE building blocks; this provided the first structural evidence for DNA rigidity within DNA assemblies. Importantly, lattice periodicity in these structures could be controlled by using four DX units instead of two. By using a reporter hairpin DX molecule (vide supra) in every fourth unit instead of every second unit (four different building blocks are used instead of the two shown in Scheme 3A), the periodicity of the lattice doubled from 33 ± 3 nm to 66 ± 5 nm. In addition to hairpin

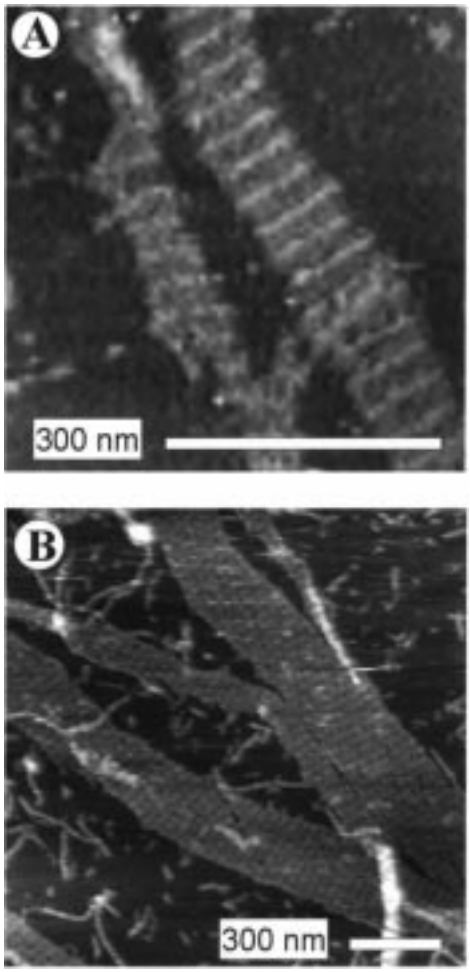

Figure 1. AFM images of two-dimensional DNA lattices prepared from the DAE double-crossover molecules shown in Scheme 3. (A) DAE two-unit lattice formed from complementary DAE building blocks **A** and **B′**. The "stripes", which represent hairpin reporter groups, have a 33 ± 3 nm periodicity; the calculated periodicity is 32 nm. (B) A larger scale image of the same sample. Image A shows a 500 nm × 500 nm scan while image B shows a 1.5 μm × 1.5 μm scan. The gray scale indicates the height above the mica surface; the apparent lattice height is between 1 and 2 nm, which correlates well with a monolayer of DNA. (Reprinted with permission from ref 59. Copyright 1998 Macmillan Magazines Limited.)

reporter groups, streptavidin-modified DAE molecules were used to form similar two-dimensional periodic DNA arrays. These arrays were used as templates to organize biotin-labeled gold nanoparticles into two-dimensional arrays through specific interactions with streptavidin. Although periodicity was observed in the AFM images of these structures, further experiments are needed to confirm the presence of nanogold within these structures. Nevertheless, this is another impressive demonstration of the complex designer structures that can be generated from oligonucleotide building blocks and an understanding of their sequence-specific binding properties.

This elegant study was the first demonstration that oligonucleotide building blocks could be used to form well-defined structures from DNA. Unlike the previous structures prepared from branched molecules, these crystalline mesoscopic materials have assignable structures both from topological and geometric

Scheme 4[a]

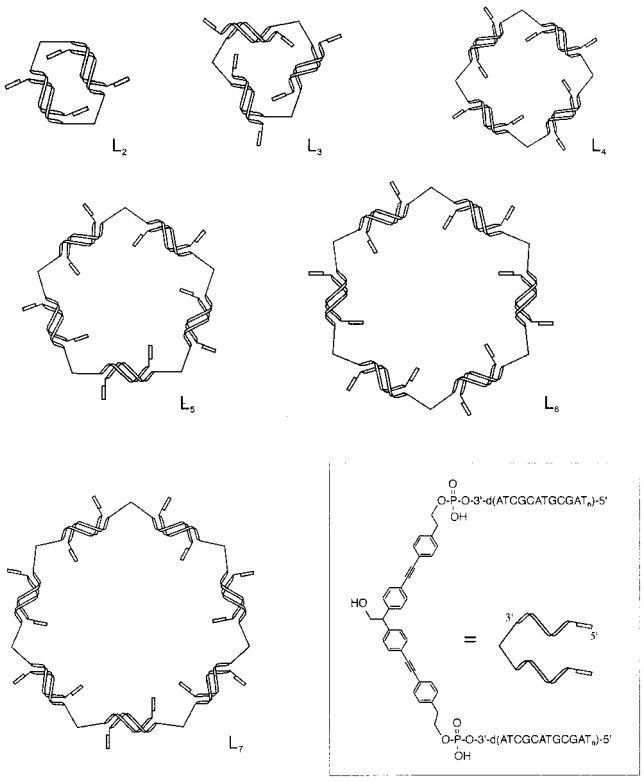

[a] Reprinted with permission from ref 60. Copyright 1997 Wiley-VCH.

standpoints and, therefore, offer tremendous opportunities for incorporating other molecular and nanoscale building blocks into designer DNA architectures.

Other researchers also have recognized the importance of using DNA to design complex architectures. Bergstrom and co-workers have designed rigid tetrahedral linkers with arylethynylaryl spacers to direct the assembly of attached oligonucleotide linker arms into novel DNA macrocycles, Scheme 4.[60] Unlike Seeman's approach where the DNA serves as both the vertices and the edges of the assembled architectures, this approach utilizes rigid tetrahedral organic vertices, where the attached oligonucleotides serve as the connectors for the design of more complex architectures. In principle, a variable number of oligonucleotide arms could be attached to the core tetrahedral organic linkers, thereby allowing for the construction of different types of DNA structures. In one study, two self-complementary oligonucleotide arms were attached to the rigid tetrahedral backbone containing two *p*-(2-hydroxyethyl)arylethynylaryl spacers, Scheme 4. Under appropriate hybridization conditions, DNA macrocycles comprised of two to seven building blocks were formed, Scheme 4. The relative amounts of each of the macrocycles formed could be controlled to an extent by varying the reaction conditions. It is important to note that, in principle, it should be possible to design organic linkers that contain oligonucleotide arms with a higher specificity thereby enabling the construction of DNA macrocycles of more well-defined size. As with many of the early designs by Seeman, it is unclear how geometrically well-defined these structures are since there is likely some flexibility within the organic backbone, and characterization of these structures is extremely difficult. This limits the utility of this strategy and the structures prepared from it for organizing other building blocks into well-defined arrays.

The current drawbacks of all of these methodologies are the low yields associated with the generation of these structures and the necessity to work under prohibitively small scale conditions. The latter is a limitation that applies to any current strategy for preparing structures solely from DNA, and until scale-up advances are made in the synthesis of oligonucleotides, the utility of such methods will be limited to very specialized materials, testing academic curiosities revolving around the linking properties of DNA, and proof-of-concept synthetic demonstrations.

III. DNA as a Template for Organizing Inorganic/Organic Building Blocks

Many strategies have been used to synthesize semiconductor particles and particle arrays.[19,61−64] Coffer and co-workers were the first to utilize DNA as a stabilizer/template to form both CdS nanoparticles and mesoscopic aggregates from them. Their original efforts were based on the use of linear duplexes of DNA in solution as a stabilizer for forming CdS nanoparticles. The nanoparticles in their first study were formed by first mixing an aqueous solution of calf thymus DNA with Cd^{2+} ions in a sub-stoichiometric quantity.[65] Then, 1 molar equiv of Na_2S was added to the solution, resulting in the formation of CdS. High-resolution transmission electron microscopy (HRTEM) confirmed the formation of polydisperse CdS nanoparticles with an average particle size of 5.6 nm. The particles exhibited optical properties characteristic of the formation of quantum-confined particles with an absorption edge of 480 nm, which is blue-shifted from bulk CdS (510 nm).

These initial results indicated that CdS nanoparticles could be formed from Cd^{2+} and S^{2-} in the presence of DNA. However, in these experiments, the role of DNA in the formation of the nanoparticles and the interactions between DNA and the particles after their formation were ambiguous.[65] Further studies demonstrated that DNA base sequence, and more specifically the content of the base adenine, had a significant effect on the size of the CdS particles formed and their resulting photophysical properties.[66] These results were suggestive of a DNA templating effect during the formation of the nanoparticles, although no direct evidence was obtained.

To overcome the problems of forming well-defined mesoscale structures in solution, Coffer and co-workers developed a new strategy for binding a template DNA strand to a solid substrate.[5] The formation of mesoscale aggregates of CdS nanoparticles using this strategy is outlined in Scheme 5. For this study, the initial target was to synthesize a "ring" of CdS nanoparticles by using the circular plasmid DNA molecule pUCLeu4 which is 3455 base pairs (bp) in length with a circumference of 1.17 μm.

Scheme 5[a]

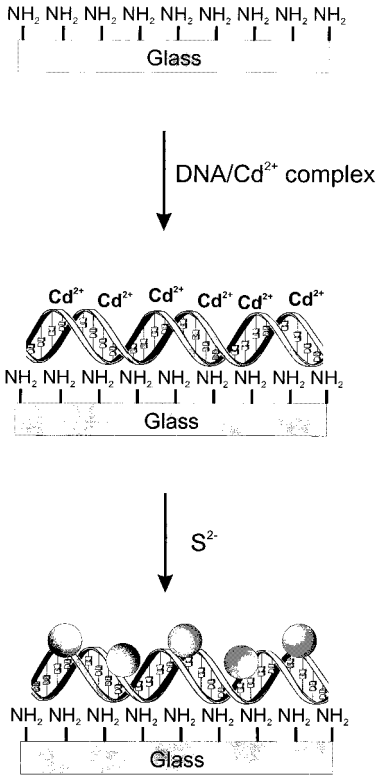

[a] Reprinted with permission from ref 61. Copyright 1997 Plenum Publishing Corporation.

Initially, Cd^{2+} ions were added to a solution containing the plasmid DNA to form a plasmid DNA/Cd^{2+} complex, which was subsequently bound to a polylysine-coated glass surface. Exposure to H_2S led to the formation of CdS nanostructures. A TEM image of a selected plasmid DNA molecule demonstrated the DNA templating effect for the formation of CdS and also showed that the plasmid DNA retained its open circular form, Figure 2A. The measured circumference of the ring (1.2 μm) closely matches the predicted value of the relaxed circular conformation of the plasmid DNA molecule (1.17 μm). An HRTEM image of a portion of the ring shows the presence of ~5 nm CdS nanoparticles along the DNA backbone with different relative orientations and spacings, Figure 2B. It is important to note that other plasmid DNA molecules with various orientations also were observed.

Through their work, Coffer and co-workers have demonstrated that DNA can be used as a template to form mesoscale structures of CdS nanoparticles. This approach provides many possibilities for synthesizing mesoscale structures since particle composition (i.e., metal, semiconductor) and shape, length, and sequence of the DNA template can be controlled. The main drawback of this approach is the difficulty of forming monodisperse nanoparticle samples since the nature of the DNA/Cd^{2+} interactions is poorly understood. In addition, the relative spacing and orientation of the resulting nanoparticles within the mesostructure are difficult to control, and consequently, tailoring and predicting the resulting properties of the materials is problematic.

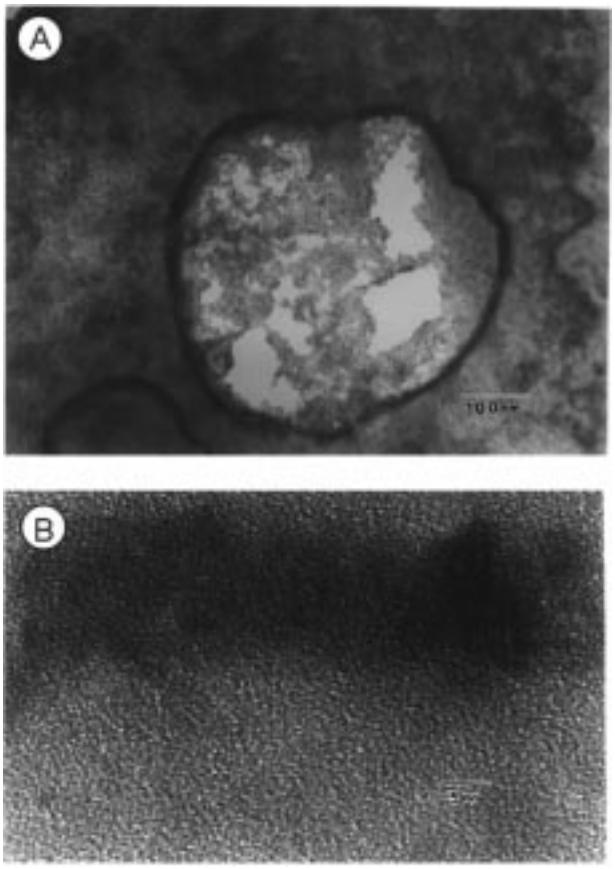

Figure 2. (A) Bright field TEM micrograph of a nanostructure formed using the circular plasmid DNA pUCLeu4 as a template for the formation of a ring of Q-CdS nanoparticles. (B) HRTEM image of one section of a different Q-CdS/DNA ring. The ring consists of numerous CdS nanoparticles with different crystallographic orientations. (Reprinted with permission from ref 5. Copyright 1996 American Institute of Physics.)

Tour and co-workers recently have taken an approach similar to that of Coffer in using DNA to assemble DNA/fullerene hybrid organic materials.[3] In their strategy, the negative phosphate backbone of DNA was used as a template to bind and organize C_{60} fullerene molecules modified with a *N*,*N*-dimethylpyrrolidinium iodide moiety into defined mesoscopic architectures, Scheme 6. Fullerenes were chosen as a complexing molecule since previous studies have demonstrated that carbon nanotubes can easily be imaged by TEM,[67] eliminating the need for other contrasting agents and stains. The modified fullerene is electrostatically complexed to the DNA backbone through cation exchange with sodium in DMSO as depicted in Scheme 6.[3] Although experiments carried out using a circular plasmid DNA molecule (ϕX174 RFII, 5386 bp) demonstrated that fullerenes could be organized into mesoscopic structures via templating and the structures could be imaged by TEM, they also suggested that the electrostatic binders significantly influenced the structure of the plasmid template. This work addresses some very important fundamental issues and limitations pertaining to the use of DNA as a scaffolding material. To effectively use DNA as a scaffolding or template material one must understand both its pre- and postfunctionalized structures.

Scheme 6[a]

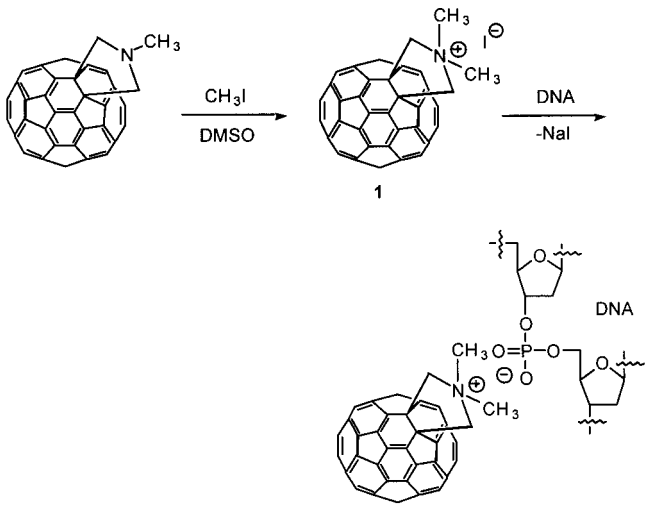

[a] Reprinted with permission from ref 3. Copyright 1998 Wiley-VCH.

Recently, Braun et al. have utilized DNA as a template to grow nanometer-scale conducting silver wires.[7] The basic assembly scheme for constructing a Ag nanowire attached to two gold electrodes is outlined in Scheme 7. Two gold electrodes separated by a defined distance (12−16 μm) were deposited onto a glass slide using photolithography. The gold electrodes subsequently were modified with noncomplementary hexane disulfide modified oligonucleotides through well-established thiol adsorption chemistry on Au.[68] Subsequently, a fluorescently labeled strand of λ DNA (16 μm in length) containing "sticky ends" that are complementary to the oligonucleotides attached to the electrodes is introduced. Hybridization of the fluorescently tagged λ DNA molecule to the surface-confined alkylthiololigonucleotides was confirmed by fluorescence microscopy, which showed a fluorescent bridge connecting the two electrodes. After a single DNA bridge was observed, the excess hybridization reagents were removed. Silver ions then were deposited onto the DNA through cation exchange with sodium and complexation with the DNA bases. This process can be followed by monitoring the quenching of the fluorescent tag on the DNA by the Ag ions. After almost complete quenching of the fluorescence, the silver ion bound to the template DNA is reduced using standard hydroquinone reduction procedures[69] to form small silver aggregates along the backbone of the DNA. A contiguous silver wire is then formed by further Ag ion deposition onto the previously constructed silver aggregates followed by reduction. Figure 3 shows an AFM image of a typical 100 nm diameter, 12 μm long wire formed by this process. The wires are comprised of 30−50 nm Ag grains that are contiguous along the DNA back-

Scheme 7[a]

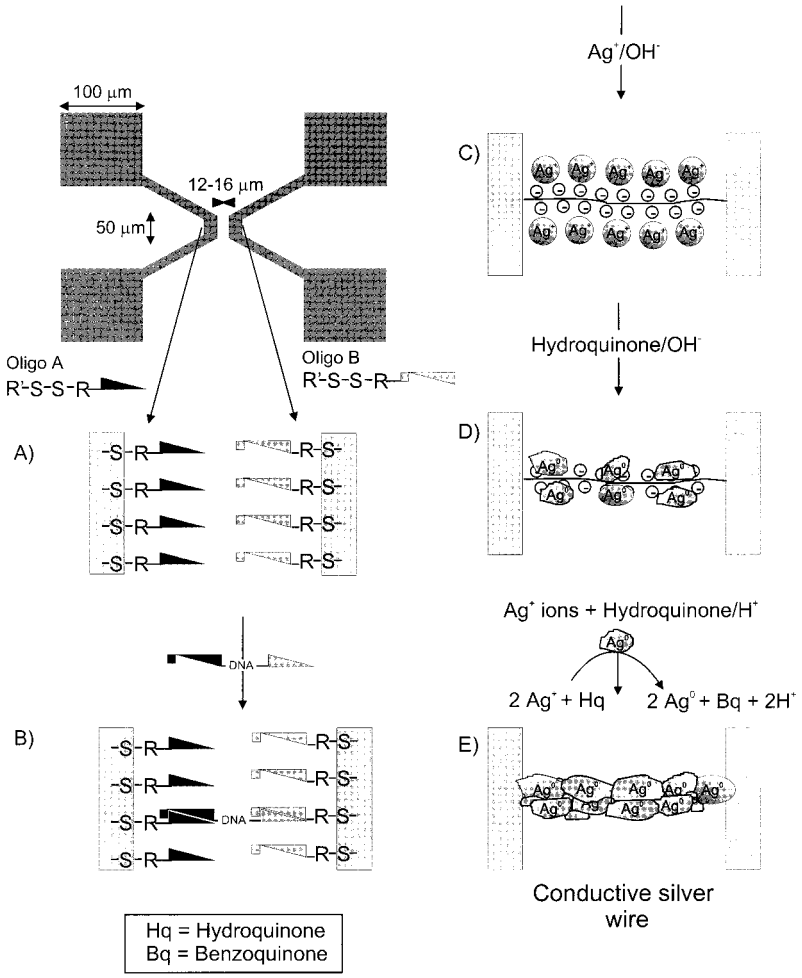

[a] Reprinted with permission from ref 7. Copyright 1998 Macmillan Magazines Limited.

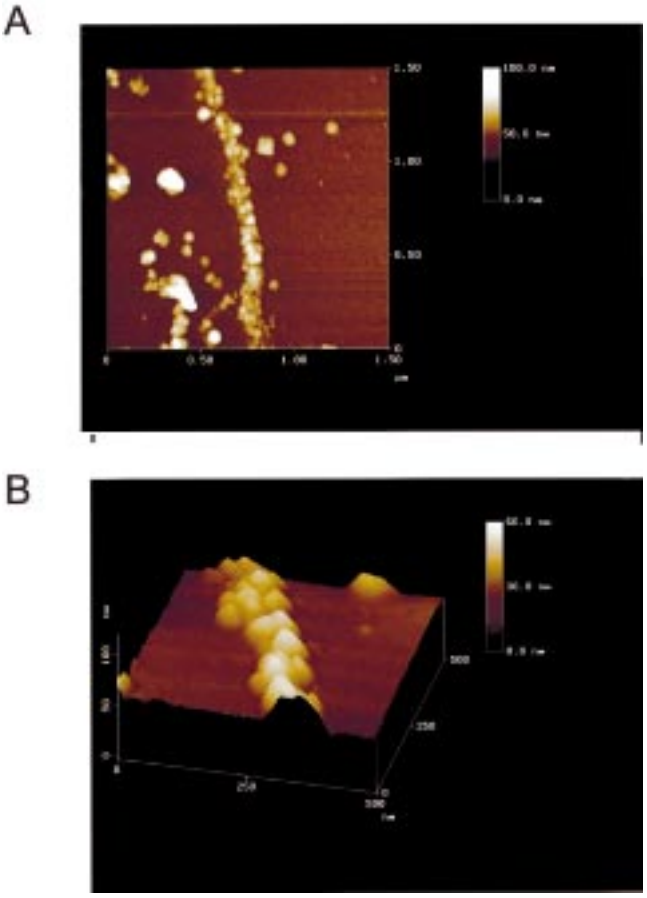

Figure 3. AFM images of a silver wire connecting two gold electrodes 12 μm apart. (A) 1.5 μm and (B) 0.5 μm field sizes. Note the granular morphology of the conductive wire. (Reprinted with permission from ref 7. Copyright 1998 Macmillan Magazines Limited.)

bone. The fabrication of narrower Ag wires (≤25 nm) resulted in discontinuous Ag structures.

Two terminal electrical measurements subsequently were performed on the Ag wire depicted in the AFM image. When the current−voltage characteristics of the Ag wire were monitored, no current was observed at near zero bias (∼10 V in either scan direction), indicating an extremely high resistance ($\geq 10^{13}$ Ω, the internal resistance of the instrument). At a higher bias, the wire becomes conductive. Surprisingly, the current−voltage characteristics were dependent on the direction of the scan rate, yielding different $I-V$ curves. Although not well-understood, it was postulated that the individual Ag grains that comprise the Ag nanowires may require simultaneous charging, or Ag corrosion may have occurred, resulting in the high resistance observed at low bias. By depositing more silver and thereby growing a thicker Ag nanowire, the no-current region was reduced from ∼10 V to ∼0.5 V, demonstrating crude control over the electrical properties of these systems. In addition, control experiments where one of the components (DNA or Ag) was removed from the assembly produced no current, establishing that all of the components are necessary to form the conducting Ag nanowires. This work, which builds off the concepts described in the next section of this review, is a proof-of-concept demonstration of how DNA can be used in a new type of "chemical lithography" to guide the formation of nanocircuitry.

IV. Nanostructured Materials Formed from Oligonucleotide Functionalized Nanoparticles and Sequence-Specific Hybridization Reactions

Although DNA is arguably one of the most versatile reagents available to the synthetic chemist, until recently it has not been extensively utilized in materials synthesis. The reason for this is primarily because synthetic forms of it are relatively expensive and not available in large quantities. For example, utilizing commercially available automated synthesizers, one can easily synthesize milligram quantities of oligonucleotides of virtually any sequence in a very straightforward fashion. However, kilogram quantities of such oligonucleotides would be prohibitively expensive for most intended applications. In addition, although there is tremendous predictive power associated with DNA hybridization events, the characterization of structures consisting only of DNA can be a very challenging task. For these reasons, many of the structures discussed in section I were synthesized in nanomole or less quantities and required extensive characterization to confirm the intended and proposed structures.

Until some of the aforementioned limitations associated with DNA as a material building block are addressed, useful materials likely will be hybrid materials that utilize DNA as a scaffold for arranging synthetically more accessible organic and inorganic building blocks. Efforts to accomplish this with duplex DNA as a structural and electrostatic template were discussed in section II. In this section, we describe efforts that focus on using single-stranded DNA to direct the formation of periodic structures from inorganic building blocks functionalized with oligonucleotides. It is important to note that other researchers have studied the interactions between DNA and nanoparticles, but these studies will not be discussed in this manuscript because the main focus is on materials synthesis.[70,71] In 1996, we reported a synthetic strategy that merged the chemistries of oligonucleotides and inorganic nanoparticles to yield designer materials consisting of nanoparticles functionalized with oligonucleotides linked by complementary DNA, Scheme 8.[1] The importance of this strategy is that it allows one to predictably arrange matter on the nanometer length scale over meso- and macroscopic distances. Because of the molecular recognition properties associated with the DNA interconnects, this strategy allows one to control particle periodicity, interparticle distance, strength of the particle interconnects, and size and chemical identity of the particles in the targeted macroscopic structure.

The first example of the synthetic utility of this strategy involved the use of 13 nm Au particles functionalized with oligonucleotides terminated with propylthiol groups in the 3′ ends, Scheme 8. The particles were designed to be noncomplementary by virtue of the oligonucleotides used to modify their surfaces. Particle linking could be effected by adding duplex DNA with sticky ends that were complemen-

Scheme 8[a]

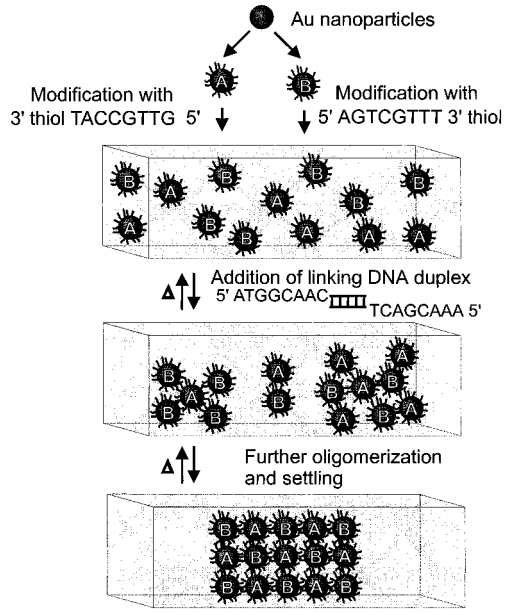

[a] Reprinted with permission from ref 19. Copyright 1997 Plenum Publishing Corporation.

tary to the Au particles, which resulted in a macroscopic network of particles held together by duplex DNA interconnects. There were several fascinating properties associated with this initial system. First, the particles could be reversibly assembled simply by cycling the temperature of the reaction vessel above and below the melting temperature of the DNA. Second, transmission electron microscopy at early stages in the assembly process revealed two types of nanostructures, small two-dimensional aggregates and larger three-dimensional structures, Figure 4. Since this discovery, we have found that one has to interpret TEM images of these types of structures with care, especially since little is known about the structure of DNA under the ultrahigh vacuum conditions of the microscopy experiment. In fact, the only way to definitively prove one has an assembled structure is to map out the melting properties of the hybrid material, which often reflect the melting properties of the DNA used to assemble it. The third unusual property of this system was the optical change that accompanied particle assembly. The plasmon band that is characteristic of Au nanoparticles is very sensitive to interparticle distance[72,73] and also to aggregate size in these systems.[74] It experiences a red shift from 520 to 600 nm as the particles are assembled by the linking DNA into extended structures, Figure 5. This results in a striking red to blue color change in the solution that can be reversed upon heating the system above the denaturation temperature of the duplex interconnects. From the initial observation of this phenomenon, it became obvious that this system could be useful for studying the factors that control the optical properties of aggregates of nanoclusters and might also be useful for colorimetrically detecting DNA.

Shortly after this initial discovery, Alivisatos et al. demonstrated that individual particles functionalized with oligonucleotides could be aligned upon a single strand of DNA based upon the sequences of the

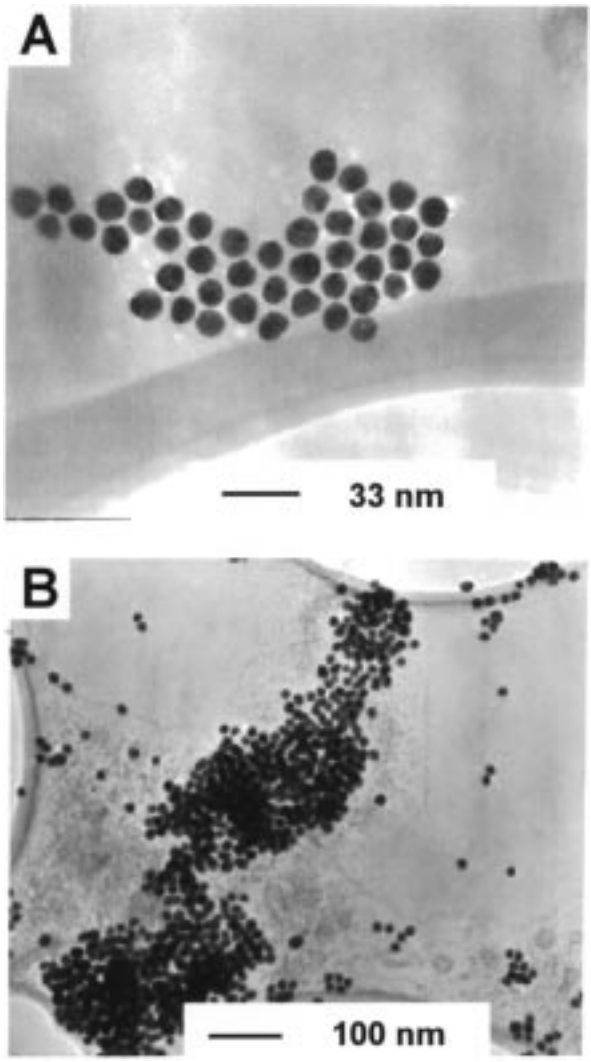

Figure 4. TEM images of (A) a two-dimensional aggregate of DNA-linked 13 nm Au nanoparticles showing the ordering of the nanoparticles and (B) a larger, three-dimensional aggregate. (Reprinted with permission from ref 1. Copyright 1996 Macmillan Magazines Limited.)

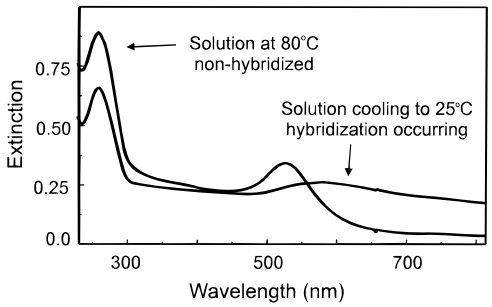

Figure 5. Comparison of UV−vis spectra from a DNA-linked Au nanoparticle solution during aggregation. Spectra were recorded at 25 °C during hybridization and at 80 °C (38 °C above the T_m of the DNA interconnects) after aggregate dissociation.

oligonucleotides attached to the particle and the oligonucleotide template, Scheme 9.[2] This type of demonstration can be thought of as one isolated elementary step in the material synthesis strategy outlined in Scheme 8. On the basis of TEM images of a series of systems studied, the authors concluded that they could align two or three 1.4 nm diameter

Scheme 9[a]

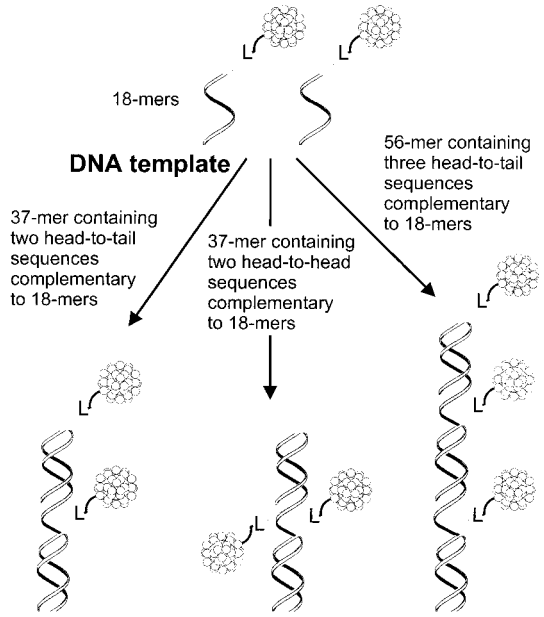

[a] Reprinted with permission from ref 19. Copyright 1997 Plenum Publishing Corporation.

particles on a single-stranded DNA template such that the particles were aligned in a "head-to-head" or "head-to-tail" fashion. Recently, Niemeyer et al. have demonstrated a variant of this templating strategy, which utilizes the molecular recognition properties of both DNA/RNA and streptavidin−biotin interactions to organize 1.4 nm Au particles.[4] In this strategy, biotinylated 1.4 nm Au particles are bound to streptavidin-modified oligonucleotides, which are subsequently organized in a "head-to-tail" fashion (see Scheme 9) onto an RNA template.

Particle periodicity within an extended meso- or macroscopic material also can be controlled via the approach outlined in Scheme 8. This has been demonstrated with 8 and 31 nm Au particles, but in principle, it can be used interchangeably with particles of virtually any composition or size as long as one can functionalize such particles with the appropriate oligonucleotide sequences, Figure 6.[6] It also has been shown that alkanethiol-derivatized Au nanoparticles of the *appropriate size ratio* will self-assemble into bimodal assemblies,[75] a phenomenon previously recognized with larger polymeric materials.[76−78] However, by using DNA-based programmed assembly methods, in principle, any set of particles with the correct oligonucleotide sequences can be arranged into such bimodal structures.

Finally, the nanostructured materials generated from the DNA-induced assembly of the oligonucleotide functionalized particles already have been applied in the development of a new and highly selec-

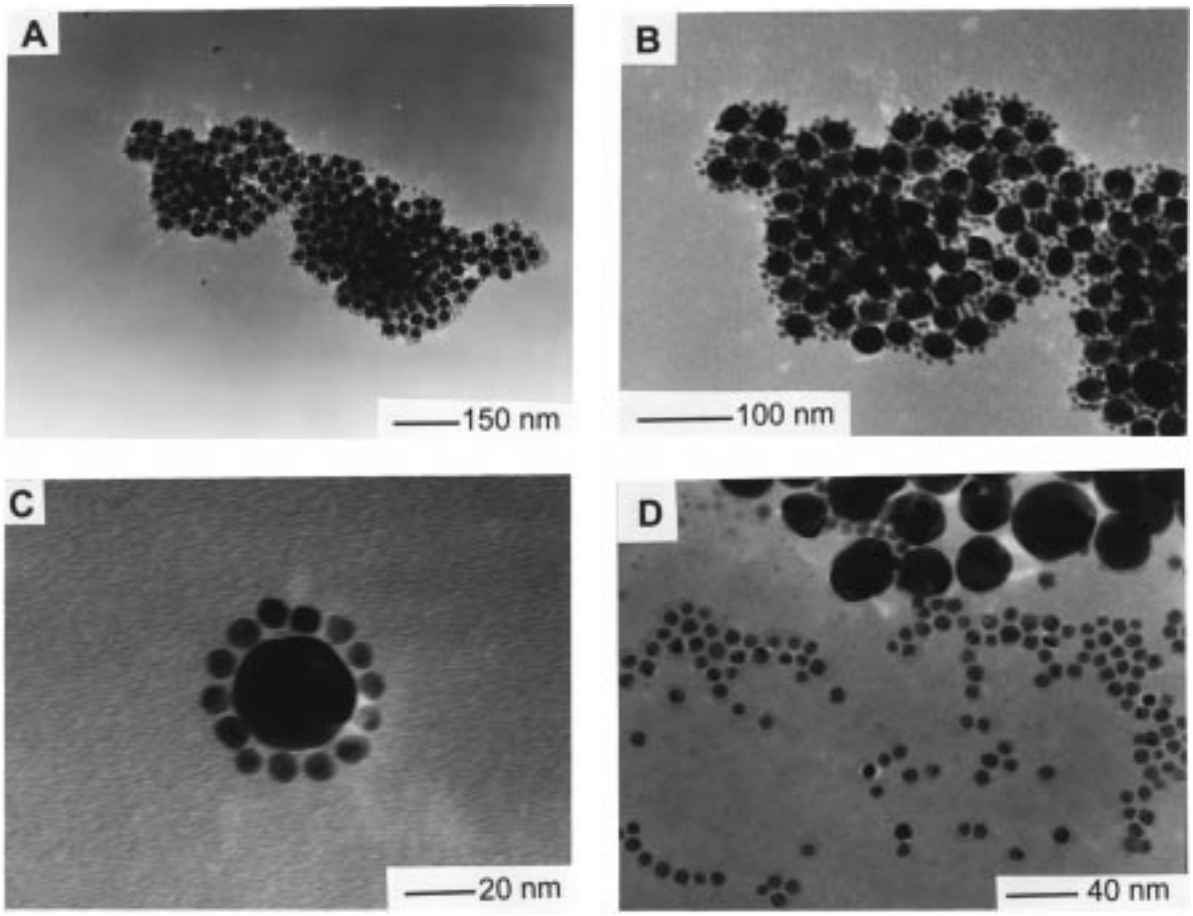

Figure 6. TEM images of binary network materials supported on holey carbon grids: (A) a DNA-linked assembly of 8 and 31 nm Au nanoparticles, (B) a smaller scale image of the DNA-linked assembly shown in A, (C) a nanoparticle "satellite structure" comprised of a 31 nm Au nanoparticle linked through DNA hybridization to several 8 nm Au nanoparticles, and (D) a control experiment containing 8 and 31 nm diameter Au nanoparticles without DNA linker, which exhibits significant particle phase segregation. (Reprinted with permission from ref 6. Copyright 1998 American Chemical Society.)

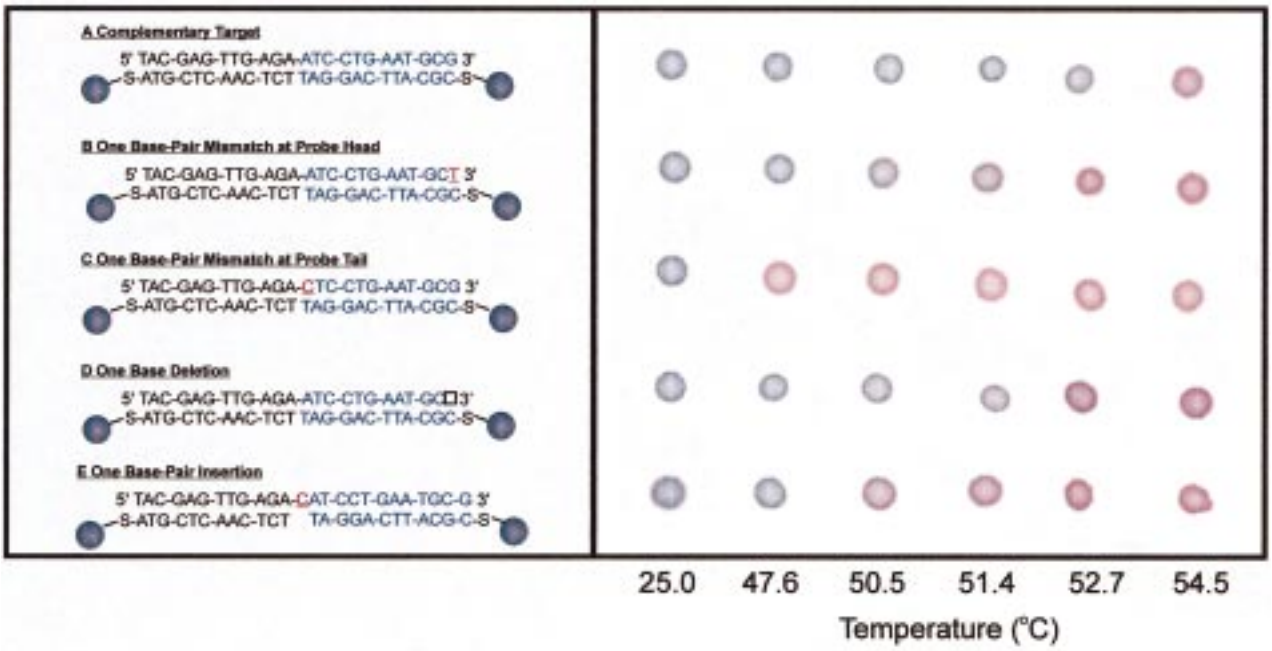

Figure 7. The "Northwestern Spot Test" for polynucleotide detection. The probes and corresponding target sequences are shown to the left of the plate. Here, a perfect target is compared with a series of imperfect targets. Portions of the target sequences which are underlined in red represent mismatched bases, blue lettering represents an inserted base, and a box represents a deletion in the polynucleotide. (Reprinted with permission from ref 9. Copyright 1998 American Chemical Society.)

tive colorimetric DNA detection method.[8,9] To understand how this assay works, the reader should view the DNA-labeled particles as probes rather than building blocks and the linking strands as target molecules. Therefore, as long as one knows the sequence of a target to be detected, one can design the appropriate nanoparticle probes. The assay involves pipetting a droplet of the solution containing the particles and target (i.e., the linking strand) to a reverse-phase silica gel plate as a function of temperature, Figure 7.[8,9] If in solution the particles are linked by the target, they form a blue spot when transported to the reverse-phase silica gel plate. If they are dispersed in solution, they form a red spot when transported to the plate, regardless of the plate temperature and the presence or absence of target. This is a critical part of the assay since in solution the particles eventually will reassemble if the target is present and the solution is below the melting temperature of the assembled nanoparticle aggregate. In this way one can monitor the "melting" behavior of the aggregates simply on the basis of color.

One of the striking features of these DNA-linked nanoparticles is their melting behavior, Figure 8. When monitored at 260 or 700 nm, the melting transition is exceedingly sharp when compared with the melting behavior of the DNA interconnects without nanoparticles. The reason for this has been attributed to two factors: (1) the formation of an aggregate with many different DNA interconnects and (2) the use of a nanoparticle optical signature rather than a DNA optical signature to map out the melting behavior of the aggregates. Indeed, when one monitors melting of the aggregates by following the absorbance changes at 260 nm, one is monitoring a signature associated with the nanoparticles rather

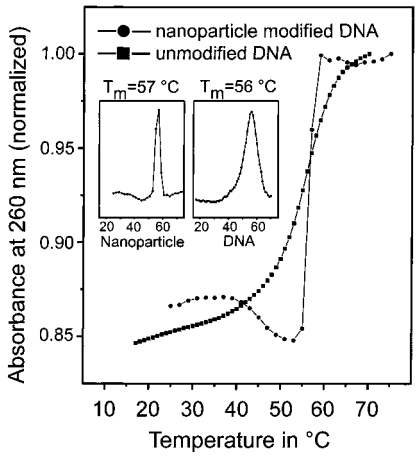

Figure 8. Comparison of the thermal dissociation curves for a DNA-linked Au nanoparticle aggregate and an unmodified DNA duplex of the same sequence. The corresponding first derivatives and T_m values are shown as insets. Note that the melting temperature is different from the system depicted in Figure 7 because different sequences and conditions were employed. (Reprinted with permission from ref 8. Copyright 1997 American Association for the Advancement of Science.)

than the DNA. Like the plasmon band at 520 nm, the absorbance at 260 nm is very sensitive to interparticle distance and aggregate size. It decreases as the aggregate grows and overshadows any changes in this region due to changes in the DNA duplex structure. In terms of melting behavior, this results in the compression of the normal denaturation temperature range of this set of strands from 12 to 4 °C (measured from the full width at half-maximum of the first derivative curve). This can be explained in the context of a nanoparticle aggregate with multiple DNA links per particle, Figure 9. For an aggregate, if one monitors a signature associated with the DNA,

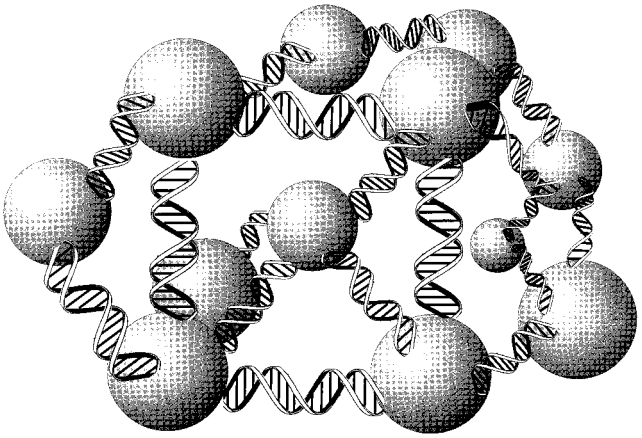

Figure 9. Schematic representation of an aggregate of Au nanoparticles linked by DNA duplexes. The DNA and nanoparticles are not drawn to scale.

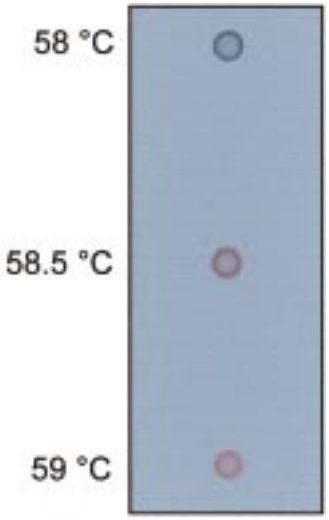

Figure 10. The sharp colorimetric transition (≤1 °C) associated with the DNA-linked Au nanoparticle aggregate dissociation process as monitored on a reverse-phase silica gel plate via the "Northwestern Spot Test". Note that the melting temperature is different from the system depicted in Figure 7 because different sequences and conditions were employed. (Reprinted with permission from ref 8. Copyright 1997 American Association for the Advancement of Science.)

any temperature-induced unraveling of the duplex will contribute to this melting transition, which results in the normal broad transition associated with duplex DNA. However, if one instead monitors an optical signature associated with the nanoparticles, the initial unraveling of the DNA duplex interconnects that hold the aggregate together will not contribute to the melting transition. The reason for this is that the size of the aggregate and the relative positions of the nanoparticles will not be affected significantly during the initial stages of the melting process. Only the final denaturation events will result in the breakup of the aggregate and concomitant optical changes. The effect is even more striking when visualized on the reverse-phase silica plate. Here, the colorimetric transition occurs over a single degree, Figure 10. Therefore, the advantages that these nanostructured materials offer in terms of DNA detection are (1) a very simple response akin to a litmus test and (2) ultrahigh selectivity. If one is trying to differentiate two oligonucleotides based upon this type of assay, it can be done providing there is at least a 1 °C difference in the melting behavior of the aggregates formed from the perfectly complementary oligonucleotide and the aggregates formed from imperfect strands (nucleotide deletions or mismatches). Indeed, it was shown that the test exhibits near-perfect selectivity when the recognition sequence is 24 nucleotides or shorter, Figure 7.[9]

What are the limitations of this DNA-based nanoparticle assembly approach? At present, only low-temperature materials are viable targets, and one must work under conditions that are conducive to DNA hybridization (e.g., polar solvents, high salt concentrations). However, there is an intense parallel research effort focused on the modification of oligonucleotide properties, which may allow one to circumvent some of these limitations.[45,79] One way to increase the stability of these materials could be through a post-cross-linking reaction. Modified DNA with cross-linkable groups such as stilbene[80] already exist and can be easily implemented in the nanoparticle programmed assembly methods described herein.[80−83] In addition, the use of peptide nucleic acids,[84] which have a higher affinity for oligonucleotides and can be used under less stringent conditions (lower temperatures and salt concentrations), also may offer a way to overcome some of the aforementioned limitations. Nevertheless, this is a new and very powerful tool for organizing nanoparticle building blocks into extended, functional two- and three-dimensional structures.

V. Conclusions

Significant headway has been made in the utilization of both single- and double-stranded DNA as a synthon or template for preparing meso- and macroscopic nanostructured materials. New, interesting, and, in some cases, useful phenomena, structures, and materials have been identified through such studies. It is clear that major advances will be made over the next few years in developing an understanding of how this novel building block can be implemented in materials synthesis. Such advances are anticipated in the area of hybrid inorganic particle/DNA structures due primarily to the fact that only surface quantities of DNA are required to prepare such materials. Indeed, the catalytic, electrical, magnetic, and electrochemical properties of such structures have yet to be systematically investigated and, therefore, represent new frontiers in this emerging field. Moreover, attempts to develop DNA driven methods of nanoparticle colloidal crystallization have not been addressed. Such studies not only will provide valuable fundamental information about the collective physical and chemical properties of particles in the context of a crystalline array but also may provide access to new and useful electronic and photonic materials applicable to the communications industry. Indeed, merging this type of assembly scheme with soft lithography methods for patterning DNA may be an especially powerful combination that will allow us to realize some of these structures and

materials.[85] If concurrent advances are made in the scale-up of synthetic oligonucleotides, the viability of structures and materials based solely on DNA will be accelerated, thereby moving the study of such structures and materials beyond the academic curiosity level.

VI. Acknowledgments

C.A.M. acknowledges the ARO-MURI (DAA 655-97-1-0133), ONR (N00014-97-1-0430), and NSF (CHE-9871903).

VII. References

(1) Mirkin, C. A.; Letsinger, R. L.; Mucic, R. C.; Storhoff, J. J. *Nature* **1996**, *382*, 607−609.
(2) Alivisatos, A. P.; Johnsson, K. P.; Peng, X.; Wilson, T. E.; Loweth, C. J.; Bruchez, M. P., Jr., Schultz, P. G. *Nature* **1996**, *382*, 609−611.
(3) Cassell, A. M.; Scrivens, W. A.; Tour, J. M. *Angew. Chem., Int. Ed. Engl.* **1998**, *37*, 1528−1531.
(4) Niemeyer, C. M.; Burger, W.; Peplies, J. *Angew. Chem., Int. Ed. Engl.* **1998**, *37*, 2265−2268.
(5) Coffer, J. L.; Bigham, S. R.; Li, X.; Pinizzotto, R. F.; Rho, Y. G.; Pirtle, R. M.; Pirtle, I. L. *Appl. Phys. Lett.* **1996**, *69*, 3851−3853.
(6) Mucic, R. C.; Storhoff, J. J.; Mirkin, C. A.; Letsinger, R. L. *J. Am. Chem. Soc.* **1998**, *120*, 12674−12675.
(7) Braun, E.; Eichen, Y.; Sivan, U.; Ben-Yoseph, G. *Nature* **1998**, *391*, 775−778.
(8) Elghanian, R.; Storhoff, J. J.; Mucic, R. C.; Letsinger, R. L.; Mirkin, C. A. *Science* **1997**, *277*, 1078−1081.
(9) Storhoff, J. J.; Elghanian, R.; Mucic, R. C.; Mirkin, C. A.; Letsinger, R. L. *J. Am. Chem. Soc.* **1998**, *120*, 1959−1964.
(10) Andres, R. P.; Bein, T.; Dorogi, M.; Feng, S.; Henderson, J. I.; Kubiak, C. P.; Mahoney, W.; Osifchin, R. G.; Reifenberger, R. *Science* **1996**, *272*, 1323−1325.
(11) Klein, D. L.; Roth, R.; Kim, A. K. L.; Alivisatos, A. P.; McEuen, P. L. *Nature* **1997**, *389*, 699−701.
(12) Livermore, C.; Crouch, C. H.; Westervelt, R. M.; Campman, K. L.; Gossard, A. C. *Science* **1996**, *274*, 1332−1335.
(13) Sato, T.; Ahmed, H. *Appl. Phys. Lett.* **1997**, *70*, 2579−2761.
(14) Freeman, R. G.; Grabar, K. C.; Allison, K. J.; Bright, R. M.; Davis, J. A.; Guthrie, A. P.; Hommer, M. B.; Jackson, M. A.; Smith, P. C.; Walter, D. G.; Natan, M. J. *Science* **1995**, *267*, 1629−1632.
(15) Nie, S. M.; Emery, S. R. *Science* **1997**, *275*, 1102−1106.
(16) Hayashi, T.; Hirono, S.; Tomita, M.; Umemura, S. *Nature* **1996**, *381*, 772−774.
(17) Hehn, M.; Ounadjela, K.; Bucher, J.-P.; Rousseaux, F.; Decanini, D.; Bartenlian, B.; Chappert, C. *Science* **1996**, *272*, 1782−1785.
(18) Holtz, J. H.; Asher, S. A. *Nature* **1997**, *389*, 829−832.
(19) Storhoff, J. J.; Mucic, R. C.; Mirkin, C. A. *J. Cluster Sci.* **1997**, *8*, 179−216.
(20) Baur, C.; Gazen, B. C.; Koel, B.; Ramachandran, T. R.; Requicha, A. A. G.; Zini, L. *J. Vac. Sci. Technol. B* **1997**, *15*, 1577−1580.
(21) Bottomley, L. A. *Anal. Chem.* **1998**, *70*, 425r−475r.
(22) Nyffenegger, R. M.; Penner, R. M. *Chem. Rev.* **1997**, *97*, 1195−1230.
(23) Giersig, M.; Mulvaney, P. *J. Phys. Chem.* **1993**, *97*, 6334−6336.
(24) Giersig, M.; Mulvaney, P. *Langmuir* **1993**, *9*, 3408−3413.
(25) Fendler, J. H. *Chem. Mater.* **1996**, *8*, 1616.
(26) Collier, C. P.; Saykally, R. J.; Shiang, J. J.; Henrichs, S. E.; Heath, J. R. *Science* **1997**, *277*, 1978−1981.
(27) van Blaaderen, A.; Ruel, R.; Wiltzius, P. *Nature* **1997**, *385*, 321−323.
(28) Ackerson, B. J.; Schatzel, K. *Phys. Rev. E* **1995**, *52*, 6448−6460.
(29) van Blaaderen, A.; Wiltzius, P. *Science* **1995**, *270*, 1177−1179.
(30) Palberg, T.; Monch, W.; Schwarz, J.; Leiderer, P. *J. Chem. Phys.* **1995**, *102*, 5082−5087.
(31) Brust, M.; Bethell, D.; Schiffrin, D. J.; Kiely, C. *Adv. Mater.* **1995**, *7*, 795−797.
(32) Grabar, K. C.; Freeman, R. G.; Hommer, M. B.; Natan, M. J. *Anal. Chem.* **1995**, *67*, 735−743.
(33) Schmid, G., Ed. *Clusters and Colloids*; VCH: Weinheim, 1994.
(34) Shenton, W.; Pum, D.; Sleytr, U. B.; Mann, S. *Nature* **1997**, *466*, 585−587.
(35) Osifchin, R. G.; Mahoney, W. J.; Bielefield, J. D.; Andres, R. P.; Henderson, J. I.; Kubiak, C. P. *Superlattices Microstruct.* **1995**, *18*, 283−289.
(36) Andres, R. P.; Bielefield, J. D.; Henderson, J. I.; Janes, D. B.; Kolagunta, V. R.; Kubiak, C. P.; Mahoney, W. J.; Osifchin, R. G. *Science* **1996**, *273*, 1690−1693.
(37) Murray, C. B.; Kagan, C. R.; Bawendi, M. G. *Science* **1995**, *270*, 1335−1338.
(38) Whetten, R. L.; Khoury, J. T.; Alvarez, M. M.; Murthy, S.; Vezmar, I.; Wang, Z. L.; Stephens, P. W.; Cleveland, C. L.; Luedtke, W. D.; Landman, U. *Adv. Mater.* **1996**, *8*, 428−433.
(39) Spatz, J. P.; Roescher, A.; Moller, M. *Adv. Mater.* **1996**, *8*, 337−340.
(40) Herron, N.; Calabrese, J. C.; Farneth, W. E.; Wang, Y. *Science* **1993**, *259*, 1426−1428.
(41) Vossmeyer, T.; Reck, G.; Schulz, B.; Katsikas, L.; Weller, H. *J. Am. Chem. Soc.* **1995**, *117*, 12881−12882.
(42) Cusack, L.; Rizza, R.; Gorelov, A.; Fitzmaurice, D. *Angew. Chem., Int. Ed. Engl.* **1997**, *36*, 848−851.
(43) Niemeyer, C. M. *Angew. Chem., Int. Ed. Engl.* **1997**, *36*, 585−587.
(44) Seeman, N. C.; Zhang, Y.; Chen, J. *J. Vac. Sci. Technol. A* **1993**, *12*, 1895−1903.
(45) Eckstein, F., Ed. *Oligonucleotides and Analogues*, 1st ed.; Oxford University Press: New York, 1991.
(46) Seeman, N. C. *Acc. Chem. Res.* **1997**, *30*, 357−363.
(47) Holliday, R. *Genet. Res.* **1964**, *5*, 282−304.
(48) Kallenbach, N. R.; Ma, R.-I.; Seeman, N. C. *Nature* **1983**, *305*, 829−831.
(49) Ma, R.-I.; Kallenbach, N. R.; Sheardy, R. D.; Petrillo, M. L.; Seeman, N. C. *Nucleic Acids Res.* **1986**, *14*, 9745−9752.
(50) Wang, Y.; Mueller, J. E.; Kemper, B.; Seeman, N. C. *Biochemistry* **1991**, *30*, 5667−5674.
(51) Chen, J.-H.; Kallenbach, N. R.; Seeman, N. C. *J. Am. Chem. Soc.* **1989**, *111*, 6402−6407.
(52) DNA ligase catalyzes the formation of a phosphodiester bond at a break in a DNA chain. Stryer, L. *Biochemistry*, 4th ed.; Freeman: New York, 1995; pp 127.
(53) Chen, J.; Seeman, N. C. *Nature* **1991**, *350*, 631−633.
(54) Zhang, Y.; Seeman, N. C. *J. Am. Chem. Soc.* **1992**, *114*, 2656−2663.
(55) Zhang, Y.; Seeman, N. C. *J. Am. Chem. Soc.* **1994**, *116*, 1661−1669.
(56) Seeman, N. C. *Annu. Rev. Biophys. Biomol. Struct.* **1998**, *27*, 225−248.
(57) Fu, T.-J.; Seeman, N. C. *Biochemistry* **1993**, *32*, 3211−3220.
(58) Li, X.; Yang, X.; Qi, J.; Seeman, N. C. *J. Am. Chem. Soc.* **1996**, *118*, 6131−6140.
(59) Winfree, E.; Liu, F.; Wenzler, L. A.; Seeman, N. C. *Nature* **1998**, *394*, 539−544.
(60) Shi, J.; Bergstrom, D. E. *Angew. Chem., Int. Ed. Engl.* **1997**, *36*, 111−113.
(61) Coffer, J. L. *J. Cluster Sci.* **1997**, *8*, 159−179.
(62) Murray, C. B.; Norris, D. J.; Bawendi, M. G. *J. Am. Chem. Soc.* **1993**, *115*, 8706−8715.
(63) Wang, Y.; Herron, N. *J. Phys. Chem.* **1991**, *95*, 525−532.
(64) Weller, H. *Angew. Chem., Int. Ed. Engl.* **1993**, *32*, 41−53.
(65) Coffer, J. L.; Bigham, S. R.; Pinizzotto, R. F.; Yang, H. *Nanotechnology* **1992**, *3*, 69−76.
(66) Bigham, S. R.; Coffer, J. L. *Colloids Surfaces A* **1995**, *95*, 211−219.
(67) Van Tendeloo, G.; Van Landuyt, J.; Amelinekx, S. In *Fullerenes: Recent advances in the chemistry and physics of fullerenes and related materials*; Kadish, K. M., Ruoff, R. S., Eds.; Electrochemical Society: Pennington, NJ, 1994; pp 498−513.
(68) Dubois, L. H.; Nuzzo, R. G. *Annu. Rev. Phys. Chem.* **1992**, *43*, 437−463.
(69) James, T. H. *J. Am. Chem. Soc.* **1939**, *61*, 648−652.
(70) Mahtab, R.; Rogers, J. P.; Singleton, C. P.; Murphy, C. J. *J. Am. Chem. Soc.* **1996**, *118*, 7028−7032.
(71) Mahtab, R.; Rogers, J. P.; Murphy, C. J. *J. Am. Chem. Soc.* **1995**, *117*, 9099−9100.
(72) (a) Kreibig, U.; Genzel, L. *Surf. Sci.* **1985**, *156*, 678−699. (b) Quinten, M.; Schonauer, D.; Kreibig, U. *Z. Phys. D* **1989**, *12*, 521−525.
(73) Yang, W.-H.; Schatz, G. C.; Van Duyne, R. P. *J. Chem. Phys.* **1995**, *103*, 869−875.
(74) Storhoff, J. J.; Mucic, R. C.; Mirkin, C. A.; Letsinger, R. L. Manuscript in preparation.
(75) Kiely, C. J.; Fink, J.; Brust, M.; Bethell, D.; Schiffrin, D. J. *Nature* **1998**, *396*, 444−446.
(76) Bartlett, P.; Ottewill, R. H.; Pusey, P. N. *Phys. Rev. Lett.* **1992**, *25*, 3801−3804.
(77) Sanders, J. V.; Murray, M. J. *Nature* **1978**, *275*, 201−203.
(78) Hachisu, S.; Yoshimura, S. *Nature* **1980**, *283*, 188−189.
(79) Beaucage, S. L.; Iyer, R. P. *Tetrahedron* **1993**, *49*, 1925−1963.

(80) Lewis, F. D.; Wu, T.; Burch, E. L.; Bassani, D. M.; Yang, J.-Y.; Schneider, S.; Jäger, W.; Letsinger, R. L. *J. Am. Chem. Soc.* **1995**, *117*, 8785−8792.
(81) Praseuth, D.; Doan, T. L.; Chassignol, M.; Decout, J.-L.; Habhoub, N.; Lhomme, J.; Thuong, N. T.; Hèléne, C. *Biochemistry* **1988**, *27*, 3031−3038.
(82) Bhan, P.; Miller, P. S. *Bioconjugate Chem.* **1990**, *1*, 82−88.
(83) Ferentz, A. E.; Verdine, G. L. *J. Am. Chem. Soc.* **1991**, *113*, 4000−40002.
(84) Uhlmann, E.; Peyman, A.; Breipohl, G.; Will, D. W. *Angew. Chem., Int. Ed. Engl.* **1998**, *37*, 2796−2823.
(85) (a) Piner, R. O.; Zhu, J.; Xu, F.; Hong, S.; Mirkin, C. A. *Science* **1999**, *283*, 661−663. (b) Xia, Y.; Whitesides, G. *Angew. Chem., Int. Ed. Engl.* **1998**, *37*, 551−575.

CR970071P